Microarray analysis reveals long non-coding RNA SOX2OT as a novel candidate regulator in diabetic nephropathy

XIAOXUE ZHANG[1*], JIN SHANG[1*], XIAOYANG WANG[1], GENYANG CHENG[1], YUMIN JIANG[2], DONG LIU[1], JING XIAO[1] and ZHANZHENG ZHAO[1]

Departments of [1]Nephrology and [2]Emergency, The First Affiliated Hospital of Zhengzhou University, Zhengzhou, Henan 450052, P.R. China

Received April 20, 2018; Accepted September 14, 2018

DOI: 10.3892/mmr.2018.9534

Abstract. Diabetic nephropathy (DN) is a highly complex syndrome involving multiple dysregulated biological processes. Long non-coding RNAs (lncRNAs) are now believed to have an important function in various diseases. However, their roles in DN remain largely unknown. Therefore, the present study was performed in order to investigate the lncRNAs that have a crucial role in DN. db/db mice were used as a DN model while db/m mice served as a control to search for lncRNAs which may have important roles in DN. Microarray and bioinformatics analysis gave an overview of the features of differentially expressed genes. Gene Ontology and Kyoto Encyclopedia of Genes and Genomes enrichment analysis demonstrated the typical biological alterations in DN. A co-expression network of lncRNAs and mRNAs revealed the complex interaction pattern in DN conditions. Further data investigation indicated that SOX2-overlapping transcript (SOX2OT), which was significantly downregulated in DN mice, may be the potentially functional lncRNA contributing to the onset of DN. The UCSC database demonstrated that SOX2OT was highly conserved in mice and humans. Additionally further study using cultured human podocytes and mesangial cells confirmed the downregulation of SOX2OT using reverse transcription-quantitative polymerase chain reaction and fluorescence *in situ* hybridization. However, the cellular location of SOX2OT depended on certain cell types. Taken together, the results of the present study indicated that SOX2OT may act as an important regulator in the pathogenesis of DN by interacting with various mRNAs with critical roles in DN.

Correspondence to: Professor Zhanzheng Zhao, Department of Nephrology, The First Affiliated Hospital of Zhengzhou University, 1 of East Jianshe Road, Zhengzhou, Henan 450052, P.R. China
E-mail: zhanzhengzhao@zzu.edu.cn

*Contributed equally

Key words: SOX2-overlapping transcript, diabetic nephropathy, microarray analysis, bioinformatics analysis

Introduction

Diabetic nephropathy (DN), as a major microvascular complication of diabetes, has become the leading cause of renal decompensation and failure worldwide (1,2). The global prevalence of type 2 diabetes contributes to an increasing number of patients developing DN and eventually end-stage renal disease, which requires renal replacement therapy. There are a number of physiological and molecular alterations in the renal microenvironment during DN, including oxidative stress, activation of certain signaling pathways, inflammation and increasing matrix accumulation (3-5). However, the underlying mechanism leading to these changes has not been fully identified. Further understanding of the molecular mechanisms involved in DN is of clinical importance in order to improve the therapeutic strategies for DN.

Long noncoding RNAs (lncRNAs) are a class of transcripts longer than 200 nucleotides without protein coding function. The mammalian genomes are replete with lncRNA genes that are engaged in numerous biological processes (6). LncRNAs differ from protein-coding genes in a number of ways. In particular, they are frequently not as conserved compared with mRNAs at the level of the primary sequence and the function of most lncRNAs remains unknown, which is why they are dismissed to be the 'dark matter' of the transcriptome. Recent studies have identified the regulatory role of lncRNA in a number of gene expression processes, including nuclear importation, alternative splicing, DNA methylation, mRNA decay, as well as other transcriptional, post-transcriptional and epigenetic regulatory roles (7,8). Although a number of lncRNA molecules have been reported to serve crucial roles in diverse diseases, only limited examples of lncRNAs have been described in DN.

In the present study, the differentially expressed genes (DEGs) were initially screened for lncRNAs and mRNAs, between db/db mice and db/m mice by microarray technique. Bioinformatics analysis identified several lncRNAs that putatively served an important role in the regulation of mRNAs involved in DN onset of db/db mice. By searching associated databases and analyzing the results SOX2OT, which has never been reported in DN was selected and focused on. SOX2OT was downregulated and highly conserved between mice and humans. Gene-lncRNA co-expression networks were

constructed to investigate the putative function and interaction patterns of SOX2OT. To study the role of SOX2OT in DN, human podocyte and mesangial cells were also cultured to determine SOX2OT expression pattern under high glucose conditions, aiming at providing novel view on DN pathogenesis and identifying novel directions for further research.

Materials and methods

Animal studies. C57BLKS/J background $Lepr^{db}/Lepr^{db}$ (db/db; n=3) and the non-diabetic control $Lepr^{db}/m$ (db/m; n=3) male mice (aged 8 weeks old; weight, 38-40 g) were bought from the Model Animal Research Center of Nanjing University (Nanjing, China). Mice were housed at 20-25˚C, a humidity of 30-60% and a 12/12 h light/dark cycle. db/db is a spontaneous diabetic model with uncontrolled high blood glucose. All rats had unrestricted access to food/water and were maintained for 20 weeks. Body weight, fasting blood glucose, urinary protein/creatinine ratio, serum creatinine and blood urea nitrogen were repeatedly measured to monitor the onset and progression of DN. At the termination of the study, mice were sacrificed under deep anesthesia prior to collecting blood (0.5-1 ml) and tissue samples. Fasting blood glucose was measured by quick sticks using tail blood. Urinary protein, serum creatinine and blood urea nitrogen were measured by the clinical laboratory of the First Affiliated Hospital of Zhengzhou University. All protocols were approved by the Institutional Animal Care and Use Committee of the First Affiliated Hospital of Zhengzhou University and conducted in accordance with the National Institutes of Health (NIH) Guide for the Care and Use of Laboratory Animals.

Cell culture and treatment. Human podocytes cells (HPCs) and human mesangial cells (HMCs) were a gift from Professor Fan Yi, Shandong University (Jinan, China). HPCs and HMCs were cultured as previously described (9,10). All cells were cultured in the Dulbecco's modified Eagle's medium supplied with 10% fetal bovine serum (both Gibco; Thermo Fisher Scientific, Inc., MA, USA) at 37˚C with 5% CO_2. High glucose (HG, final concentration 30 mM in culture medium) was used in the present study and the same concentration of mannitol was used as an osmolality control.

Hematoxylin-eosin and periodic Acid-Schiff staining. Tissue samples of renal cortex were fixed in buffered formaldehyde solution for 24 h at room temperature, dehydrated and embedded in paraffin wax. Sections were cut (4 μM) and stained with hematoxylin-eosin (HE; OriGene Technologies, Inc., Beijing, China) and Periodic Acid-Shiffs (PAS, Solarbio Science and Technology Co., Ltd., Beijing, China) reagent. In HE staining, samples were treated with hematoxylin for 8 min and 1% ethanol eosin for another 3 min. In PAS staining, slices were oxidized by 0.5% periodic acid for 7 min and soak in 0.5% sodium metabisulfite for 1 min. Sections were mounted by neutral balsam (11,12). Images were captured by Leica Microsystems GmbH, (Wetzlar, Germany).

Transmission electron microscopy observation. Ultramicrostructure of the basement membrane region was observed by transmission electron microscopy (TEM) (13). Tissues for TEM observation were fixed in 2% glutaraldehyde/2% paraformaldehyde in 0.1 mol/l phosphate buffer for >24 h at room temperature, post-fixed in buffered osmic acid, dehydrated in graded alcohols and embedded in an Epon 812 mixture overnight at room temperature. Semi-thin sections (2 μm) were rinsed overnight in 0.1 M phosphate buffer, post-fixed for 2 h in 1% osmium tetroxide at room temperature, dehydrated and then embedded in Araldite mixture. Ultrathin sections were stained with uranyl acetate at room temperature for 15 min and lead citrate at room temperature for 25 min, and then examined with a CM10 transmission electron microscope (Philips Medical Systems B.V., Eindhoven, The Netherlands).

Microarray analysis. Agilent SurePrint G3 Mouse Gene Expression v2 8x60K kit, which could scan the signals of 27122 Entrez Gene RNAs and 4578 lncRNAs, was used in the present study. Total RNA of the renal cortex of the mice was extracted and purified using mirVana™ miRNA Isolation kit (cat. no. AM1561; Ambion; Thermo Fisher Scientific, Inc.) and checked for a RNA integrity Number (RIN) to inspect RNA integration by an Agilent Bioanalyzer 2100 (Agilent Technologies, Inc., Santa Clara, CA, USA). Total RNA was amplified and labeled by Low Input Quick Amp Labeling kit, One-Color (cat. no. 5190-2305; Agilent Technologies, Inc.). Labeled cRNA were purified using an RNeasy mini kit (cat. no. 74106; Qiagen, GmBH, Germany). Each slide was hybridized with 600 ng Cy3-labeled cRNA using Gene Expression Hybridization kit (cat. no. 5188-5242; Agilent Technologies, Inc.). Following 17 h hybridization, slides were washed in staining dishes (cat. no. 121; Thermo Fisher Scientific, Inc.) with Gene Expression Wash Buffer kit (cat. no. 5188-5327, Agilent Technologies, Inc.). Slides were scanned by Agilent Microarray Scanner (cat. no. G2565CA; Agilent Technologies, Inc.) with default settings. Data were extracted with Feature Extraction software 10.7 (Agilent Technologies, Inc.). All experiments were performed according to the manufacturer's protocols (14).

Reverse transcription-quantitative polymerase chain reaction (RT-qPCR) analysis. Total RNA of the renal cortices of the mice was extracted using TRIzol solution (Takara Biotechnology Co., Ltd., Dalian, China). Then total RNA was quantified using a Nanodrop 2000 spectrophotometer (Thermo Fisher Scientific, Inc.). A total of 1 μg of RNA was used for cDNA synthesis using PrimeScript RT Master Mix (Perfect Real Time) kit (Takara Biotechnology Co., Ltd.). The temperature protocol for RT was 37˚C for 15 min followed by 85˚C for 5 sec. SYBR Premix Ex Taq kit (Takara Biotechnology Co., Ltd.) was used to evaluate the lncRNA and mRNA expression (15). RT-qPCR was performed in a StepOnePlus Real-Time PCR System (Applied Biosystems; Thermo Fisher Scientific, Inc.). The specific primers of target genes used were as follows: Mus Klk1b7-ps forward, 5'-GTG TGA ACC TCA AGC TCC TG-3' and reverse, 5'-CTG AGT CTC CCT TGC AAG TG-3'; Mus Suv39h2 forward, 5'-TGT GTG CCT TGC CTA GTT TC-3' and reverse, 5'-CCA CAC CCT TTG CTA CCT TG-3'; Mus Ubtf forward, 5'-TGC GGT TCC TTG AGA GCT TG-3' and reverse, 5'-CAC CCT TGC CAC CTT CCT G-3'; Mus Pkib forward, 5'-TGG CCG TGA AGG AAG ATG C-3' and reverse, 5'-ACT ACC AGA TCA AAC ACC CC-3'; Mus 1700112J16Rik forward, 5'-TGA CCC AGA TAT CAG TGC TC-3' and reverse, 5'-TGT CTC TTC CTG TTC TGG TC-3'; Mus Gm15217 forward, 5'-TGG ATC ACA AGG ACC

Table I. Data of mice at the end point of the experiment.

Parameter	Control (n=3)	DN (n=3)	P-value
Body weight (g)	23.27±0.30	39.20±0.35	<0.0001
Fasting blood glucose (mmol/l)	7.367±0.26	30.33±1.44	<0.0001
Urinary protein/creatinine ratio (g/g)	1.477±0.12	13.32±1.80	0.0028
Serum creatinine (μmol/l)	33.30±3.30	41.47±1.38	0.0842
Blood urea nitrogen (mmol/l)	8.627±0.47	13.38±0.25	0.0009

Control, nondiabetic db/m mice; DN, diabetic db/db mice. P<0.05 is considered as statistically different between two groups. Values are presented as the mean ± standard deviation.

CCAGT-3' and reverse, 5'-GAACCAAATCCAACGGAG AC-3'; Mus Pvt1 forward, 5'-AGAGCTGGTAGGAGACAG AC-3' and reverse, 5'-TCTGCCAGCTCCTTCTTCAC-3'; Mus Hbegf forward, 5'-CTCCCTCTTGCAAATGCCTC-3' and reverse, 5'-AGTACTACAGCCACCACAGC-3'; Mus Hsd11b1 forward, 5'-GAGTTCAGACCAGAAATGCTC-3' and reverse, 5'-AGACACTACCTTCTGGAGAC-3'; Mus Sox2ot forward, 5'-CCGAGAAGCAAACCTGACAG-3' and reverse, 5'-AGTCTCTCCCATCAGCGTC-3'; Homo LncR-SOX2-OT forward, 5'-AGACAATGAGCTGGCACC AC-3' and reverse, 5'-AGGCAAGGTCAGAGACATAG-3'. Housekeeping gene GAPDH was used as an endogenous control for normalization of RNA quantity differences. The cycling conditions were as follows: 95˚C for 30 sec, 40 cycles at 95˚C for 5 sec and then 60˚C for 30 sec. All reactions were carried out in triplicate. Relative expression of gene levels were quantified using the $2^{-\Delta\Delta Cq}$ method (16).

Gene ontology (GO) and pathway enrichment analysis. GO enrichment analysis was performed to categorize the differentially expressed mRNAs based on biological processes, molecular functions and cellular components. The Kyoto Encyclopedia of Genes and Genomes (KEGG) database was used to investigate the enriched pathways of aberrantly expressed mRNAs (17,18). P<0.05 was considered to indicate a statistically significant difference.

Co-expression of lncRNAs and mRNAs. Currently most lncRNAs have not been functionally annotated. Therefore, their functions were predicted on the basis of the functional annotations of their co-expressed mRNAs. Pearson coefficients (PC) were used to construct a network of lncRNAs and mRNAs. Pair-wise PC of genes (e.g., lncRNA and lncRNA, lncRNA and mRNA, mRNA and mRNA) were used to construct networks using Cytoscape 3.5.1 (www.cytoscape.org) using the following steps: i) Choose interactions of lncRNA and mRNA to construct initial networks (P<0.001), genes presented in network were considered as 'existed'. ii) Simultaneously import interactions of existed 'lncRNA and lncRNA', existed 'mRNA and mRNA' into initial networks (P<0.001).

Fluorescence in situ hybridization (FISH). To detect lncRNA SOX2OT expression pattern of HPC and HMC under normal or HG-stimulation conditions, FISH was performed as previously described (19). The probe and kit for FISH was purchased from Guangzhou RiboBio Co., Ltd., (Guangzhou, China). Cultured HPCs and HMCs were fixed in paraformaldehyde for 10 min at room temperature and incubated in Triton X-100 for 5 min. Non-specific binding sites were blocked using pre-hybridization buffer for 30 min at 37˚C. A biotin-labeled SOX2OT probe was used at 5 nM. Images were observed and captured using a fluorescence microscope (Leica Microsystems GmbH).

Statistical analysis. Data are reported as the mean ± standard deviation. Experiments were performed in triplicate. One-way analysis of variance followed by Duncan's multiple range test were used to check the significance of the differences in mean values. Statistical analyses were performed with GraphPad Prism 5.0 (La Jolla, CA, USA). P<0.05 was considered to indicate a statistically significant difference in microarray analysis and if fold-changes were >2 or <0.5, P values were corrected by the Benjamini-Hochberg false discovery rate method using R software (version 3.5.1; https://www.r-project.org/).

Results

Metabolic and pathological characteristics of db/db mice. Table I described detailed laboratory alterations of the mice at the end of the study. The db/db mice demonstrated higher body weight, fasting blood glucose and urinary protein level compared with the db/m group (P<0.05). Serum creatinine level and blood urea nitrogen also increased compared with the db/m mice. However, the serum creatinine level was not statistically significant. HE staining, PAS staining and TEM (Fig. 1A) were used for morphological diagnosis of DN. Db/db mice exhibited foot process enfacement of podocytes, thickening of the basement membrane and expansion of the mesangial matrix. All these results indicated that a successful DN model of db/db mice had been achieved.

Microarray analysis reveals the DEGs of db/db mice compared with db/m mice. The microarray gene chip data demonstrated 11,673 DEGs in db/db mice compared with db/m mice. A total of 5,233 genes were upregulated while 6,440 were downregulated. Further study demonstrated 1,568 DEGs with fold-change >2.0. Among those, 777 were consistently upregulated and 791 were consistently downregulated. A hierarchically clustered heat map is presented in Fig. 1B. Sec14l3 (NM_001029937) and Gm6300 (NR_033591) were the most downregulated mRNA and lncRNA, with

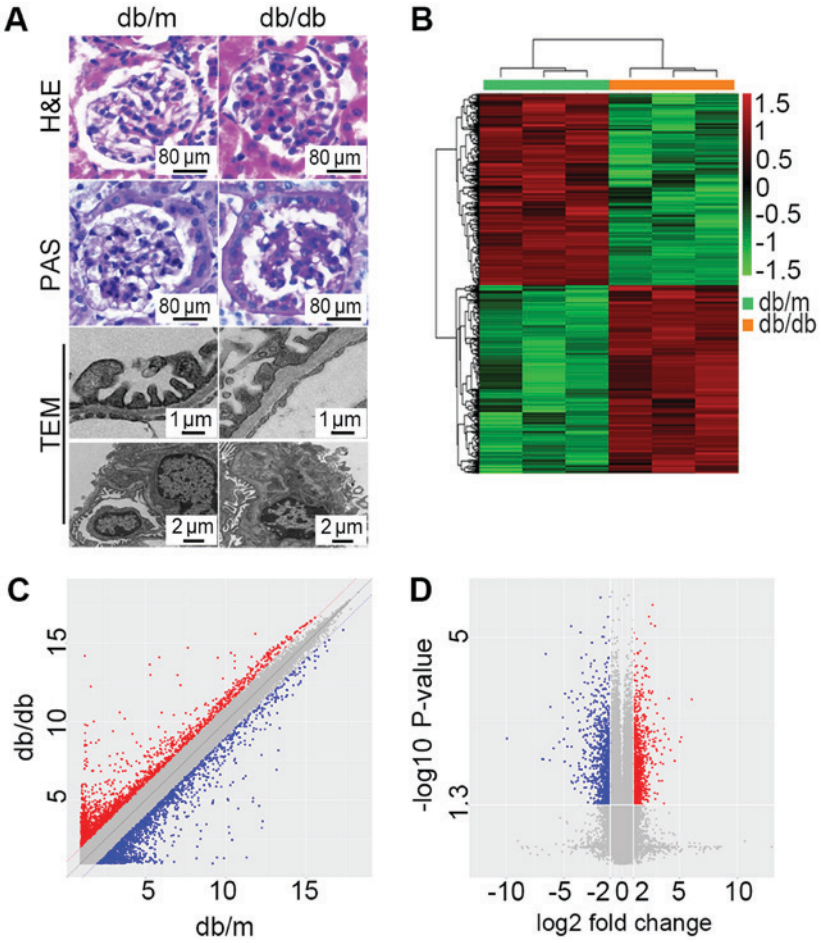

Figure 1. Microarray analysis revealed DEGs between db/db mice and db/m mice. (A) Representative morphological alterations, including H&E staining, PAS base staining and TEM inspection, in the renal cortex from db/m (n=3) and db/db (n=3) mice. Scale bars are presented in each graph. (B) Hierarchically clustered heat map of DEGs with absolute fold-changes of no less than 2.0. The vertical axis represents each mRNA or long noncoding RNA and the horizontal axis represents different groups. (C) A scatter plot exhibiting the DEGs between db/db mice and db/m mice. (D) A volcano plot exhibiting statistically significant DEGs (fold-change ≥2.0, P<0.05). DEGs, differentially expressed genes; PAS, periodic Acid Schiff; H&E, hematoxylin and eosin; TEM, transmission electron microscopy; db/db, $Lepr^{db}/Lepr^{db}$.

an absolute fold-change of 118.84 and 59.97, respectively. Hmgcs2 (NM_008256) and Rdh18-ps (NR_037604) were the most upregulated mRNA and lncRNA with fold-changes of 23.81and 5.13. Detailed DEGs of mRNAs and lncRNAs with the greatest change are listed in Table II. The scatter plot (Fig. 1C) presents variations in DEGs expression between the two groups. Significant expression differences can be seen. The volcano plot (Fig. 1D) was presented to visualize the DEGs with statistical significance (fold-change ≥2.0, P<0.05).

GO and pathway enrichment analysis of differently expressed mRNAs. GO analysis (Fig. 2A) was performed in order to investigate the important biological processes, cellular components and molecular functions involved in the onset of DN. The most enriched biological process was the glutathione biosynthetic process. Glucuronic and flavonoid associated processes were also enriched, including glucoronate metabolic processes, cellular glucuronidation, flavonoid metabolic processes, flavonoid glucuronidation and flavonoid biosynthetic processes. Chylomicron was the most enriched cellular component. The most enriched molecular functions were inorganic anion exchanger activity and sodium-independent organic anion transmembrane transporter activity.

The top 30 enriched pathways are presented in Fig. 2B. The most enriched pathway was biotin metabolism. However, it only contained one DEG (OXSM). Cytochrome P450-associated pathways were enriched, including metabolism of xenobiotics by cytochrome P450 and drug metabolism-cytochrome P450. Certain well-known pathways that are associated with the onset and progression of DN could also been observed, including the renin-angiotensin system, PPAR signaling pathway, glutathione metabolism biosynthesis of unsaturated fatty acids and arachidonic acid metabolism.

It is notable that in GO and pathway enrichment analysis demonstrated alterations in steroid associated enrichment, suggesting that steroid hormone disorder may also participate in the onset of DN.

Differentially expressed lncRNA and mRNA have close associations. Of all these DEGs, 880 mRNAs (335 were upregulated and 545 were downregulated) and 60 lncRNAs (30 were upregulated and 30 were downregulated) were annotated. Hierarchically clustered heat maps are presented in Fig. 3A and B. To predict the function of differential lncRNAs, PCs of each pair of differentially expressed lncRNAs and mRNAs were calculated for the first step. The association of

Table II. Top 10 down and upregulated mRNAs and lncRNAs (db/db compared with db/m. Only genes with Accession number started with 'NM' or 'NR' are listed here).

mRNAs			lncRNAs		
Gene symbol	Fold-change	Accession	Gene symbol	Fold-change	Accession
Sec14l3	0.008	NM_001029937	Gm6300	0.017	NR_033591
Slco1a1	0.010	NM_013797	Sox2ot	0.031	NR_015580
Slc22a7	0.013	NM_144856	Gm1653	0.042	NR_040591
Masp2	0.014	NM_010767	0610031O16Rik	0.080	NR_045760
Cyp7b1	0.029	NM_007825	Carlr	0.084	NR_131254
Col19a1	0.033	NM_007733	Gm15350	0.157	NR_045775
Mfsd2a	0.038	NM_029662	B230323A14Rik	0.172	NR_040765
Gm853	0.048	NM_001034872	Airn	0.205	NR_027773
Alox15	0.049	NM_009660	Gm10433	0.255	NR_045282
Akr1c18	0.053	NM_134066	5830418P13Rik	0.260	NR_040466
Bhmt	9.729	NM_016669	Gm16796	2.884	NR_040367
Qrfpr	10.291	NM_198192	1700110I01Rik	2.920	NR_038059
Chrdl2	12.088	NM_133709	2310069G16Rik	2.954	NR_040309
Grem1	12.562	NM_011824	Zfp133-ps	2.966	NR_033459
Kynu	12.672	NM_027552	A530006G24Rik	3.089	NR_046014
Gm10639	13.540	NM_001122660	A930001A20Rik	3.101	NR_040549
Gsta2	16.617	NM_008182	I730030J21Rik	3.270	NR_045781
Cry1	16.772	NM_007771	BB123696	3.466	NR_027893
Cyp4a14	18.634	NM_007822	Klk1b7-ps	4.188	NR_033120
Hmgcs2	23.780	NM_008256	Rdh18-ps	5.131	NR_037604

lnc, long non-coding.

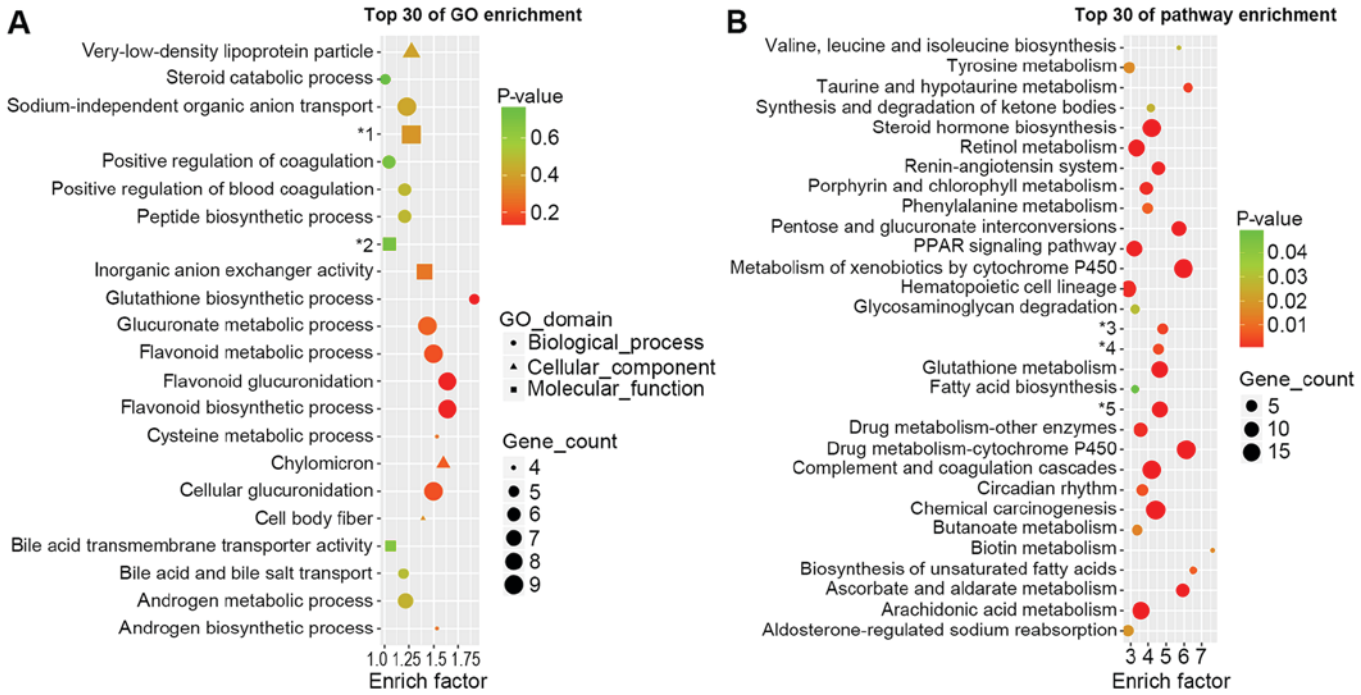

Figure 2. GO and KEGG analysis of differentially expressed mRNAs. (A) Major alterations in mRNA expression were categorized into biological processes, cellular component and molecular function by GO enrichment analysis. (B) KEGG analysis demonstrating the most enriched alterations in complex cellular pathways. *1: Sodium-independent organic anion transport. *2: Oxidoreductase activity, acting on the CH-NH2 group of donors. *3: Glycosaminoglycan biosynthesis-heparan sulfate/heparin. *4: Glycosaminoglycan biosynthesis-chondroitin sulfate/dermatan sulfate. *5: Endocrine and other factor-regulated calcium reabsorption. GO, gene ontology; KEGG, Kyoto encyclopedia of genes and genomes.

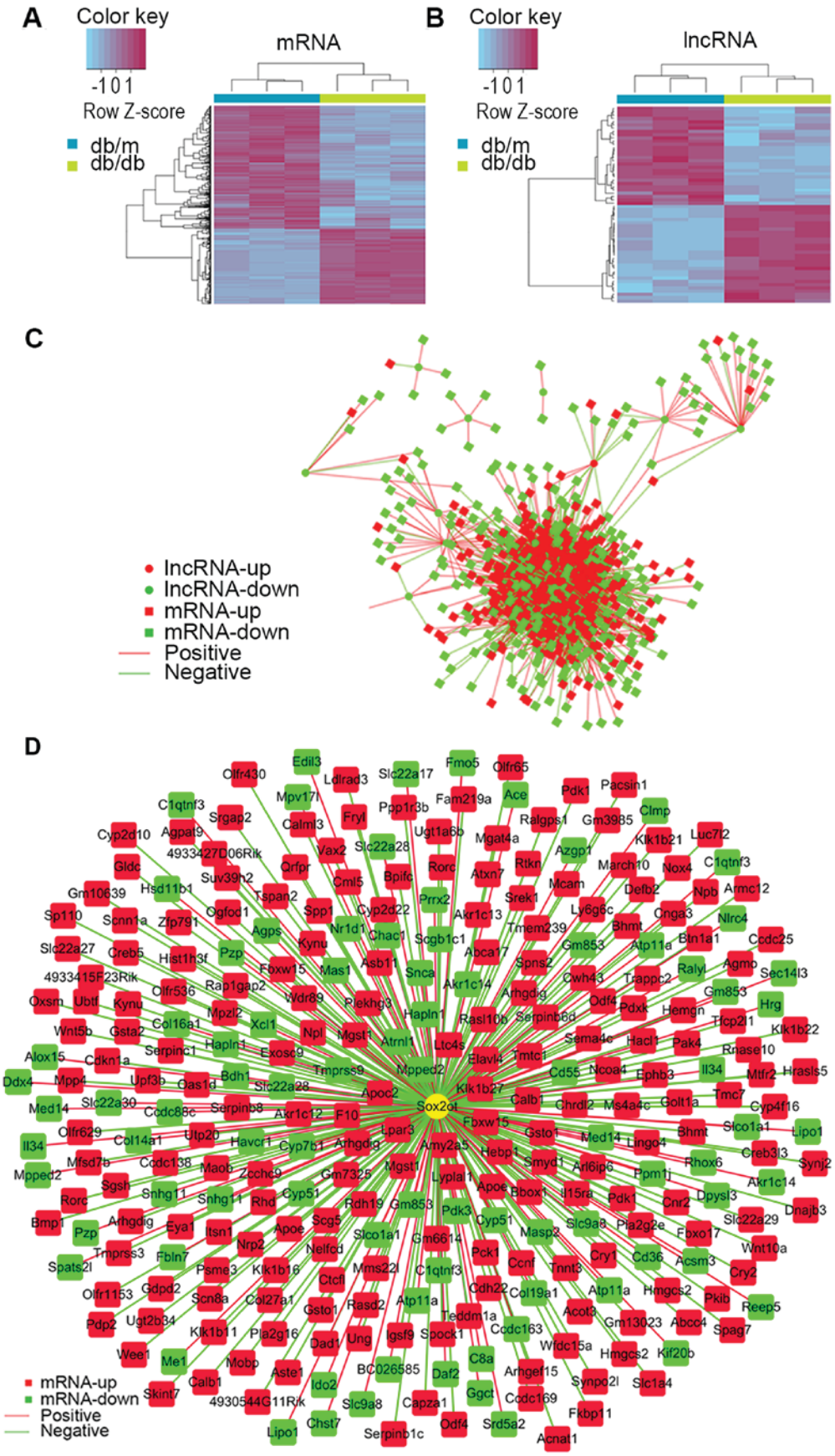

Figure 3. lncRNA and mRNA correlation analysis revealed potential connections between them. Hierarchically clustered heat map of (A) mRNA and (B) lncRNA with fold-changes no less than 2.0 between db/db and db/m mice. The vertical axis represents each mRNA or lncRNA and the horizontal axis represents different groups. (C) Interaction network of lncRNA and mRNA were constructed using Pearson Coefficients ($P \leq 0.001$). (D) Interaction network of SOX2OT and its associated genes were constructed using the same method. Circles denote lncRNA and rectangles denote mRNA. Red is enriched in the db/db group and green is enriched in the db/m group. Red edges denote positive interactions and green edges denote negative interactions. Lnc, long noncoding; SOX2OT, SOX2-original transcript; db/db, $Lepr^{db}/Lepr^{db}$.

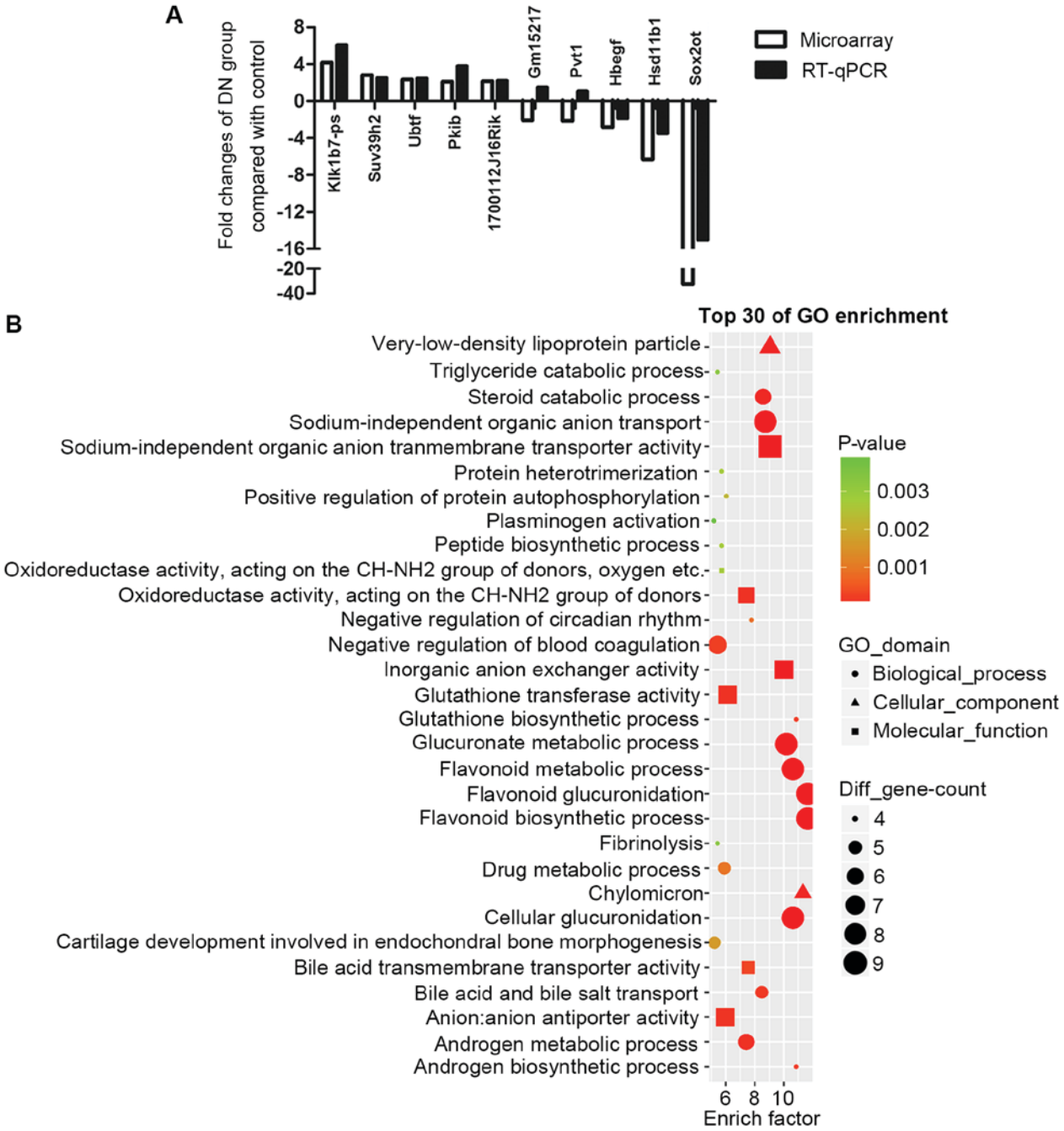

Figure 4. Validation of microarray results by RT-qPCR and analysis of SOX2OT function by GO enrichment. (A) Certain mRNAs and highly conserved long noncoding RNAs according to UCSC were chosen for RT-qPCR validation. Results demonstrated consistency between these two methods except for Gm15217 and Pvt1. (B) All the SOX2OT-associated mRNAs were analyzed in GO enrichment. Glutathione metabolic, oxidoreductase activity, flavonoid metabolic and lipid metabolic processes are enriched. RT-qPCR, reverse transcription quantitative polymerase chain reaction; GO, gene ontology; DN, diabetic nephropathy; SOX2OT, SOX2 original transcript.

lncRNAs and mRNA were constructed and intensive correlations (P≤0.001) between them are demonstrated as network in Fig. 3C, indicating lncRNAs may perform their function via interacting with associated mRNAs. To get a better view of the gene network of SOX2OT the lncRNA of interest, a SOX2OT-centered network was constructed (Fig. 3D).

RT-qPCR validation of DEGs. First, the UCSC database was searched to check the homology of all differentially expressed lncRNAs (fold-change>2.0). Highly homologous lncRNAs were chosen for the RT-qPCR validation, including Pvt1, SOX2OT, Gm15217, Klk1b7-ps and 1700112J16Rik. Certain other randomly picked differentially expressed mRNAs, including: Ubtf, Pkib, Suv39h2, Hsd11b1 and Hbegf, were also included in RT-qPCR validation. Fig. 4A demonstrates that most of the results of RT-qPCR were consistent with microarray results. Out of these 5 lncRNAs, Pvt1 and SOX2OT have already been reported to exist in humans (20,21). Notably, SOX2OT is the most markedly downregulated gene, with a fold-change of -32.

SOX2OT may have an important role in DN. From Fig. 4A, SOX2OT was identified to be the most dysregulated lncRNA

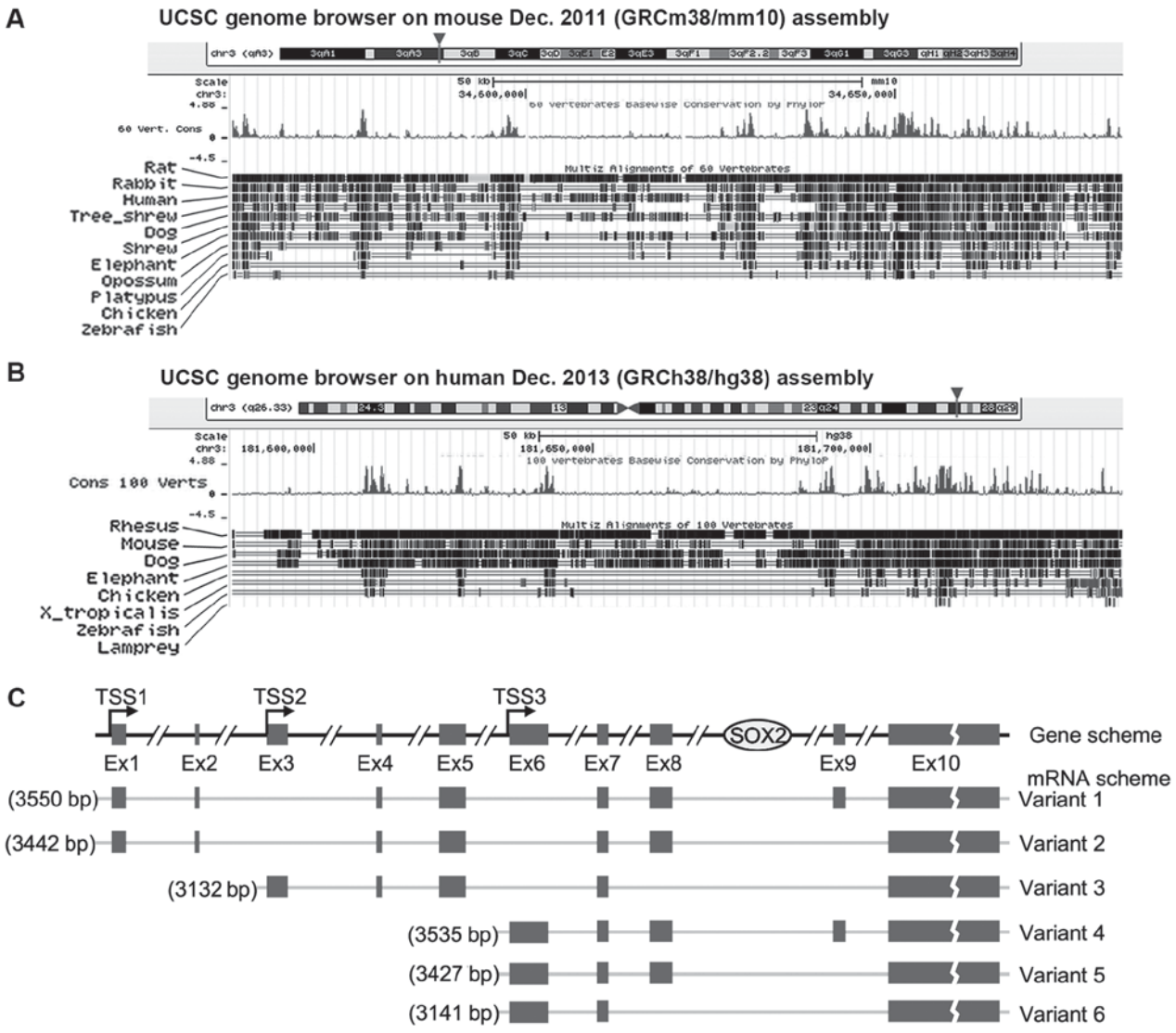

Figure 5. Genome structure and conservation analysis of SOX2OT. Genome structure of SOX2OT in mice (A) and humans (B) demonstrating the gene location and conservation sites between species. Data were downloaded from http://genome.ucsc.edu. (C) The structure diagrams of SOX2OT variants according to NCBI database. TSSs, transcription starting sites; Ex, exon; SOX2OT, SOX2 original transcript.

which may have an important function in DN. However, to the best of our knowledge, its role in DN has never been reported previously. One way of investigating the role of an lncRNA in a certain disease is to study their putative co-expressed mRNAs. All the SOX2OT-associated mRNAs were analyzed in GO enrichment (Fig. 4B). Notably, results demonstrated a very similar expression pattern to that presented in Fig. 2A. Those enriched biological processes in DN, including glutathione biosynthetic processes, glucuronic and flavonoid associated processes, chylomicron, and androgen metabolic processes were also enriched in SOX2OT-associated mRNAs. These results indicated that, by serving a central part in dysregulated biological processes, SOX2OT may have a critical role in DN.

SOX2OT is highly conserved between mice and humans. Since SOX2OT is evolutionarily conserved (22) and was the most altered lncRNA in the present study, SOX2OT was investigated in the present study. The gene structure of SOX2OT in mouse and human from UCSC is presented in Fig. 5A and B. SOX2OT is located on chromosome 3 in the two species and it overlaps with mRNA encoding gene SOX2. Conservation tracking demonstrates that SOX2OT is highly conserved between different vertebrates, especially in mice and humans. SOX2OT has a number of transcript variants. Human variants 1-6 have been documented in the NCBI database and the structure diagrams are presented in Fig. 5C. A total of three transcription starting sites (TSSs) are demonstrated and between Ex (exon) 8 and 9, which is where SOX2 resides.

Expression pattern of SOX2OT in HPCs and HMCs. Since podocytes and mesangial cells are the two main types of cells functionally associated with the onset of DN, HPCs and HMCs were cultured to check SOX2OT expression. HG (30 mM for 24 h) could significantly downregulate SOX2OT expression compared with the control group (P=0.0006 in HPC group and 0.0043 in HMC group, Fig. 6A). This suggested that SOX2OT may have the same expression pattern and function in human podocytes and HMCs as that in mice. Then FISH was performed (Fig. 6B). Results demonstrated consistently weakened signal in HG-stimulated HPCs and HMCs.

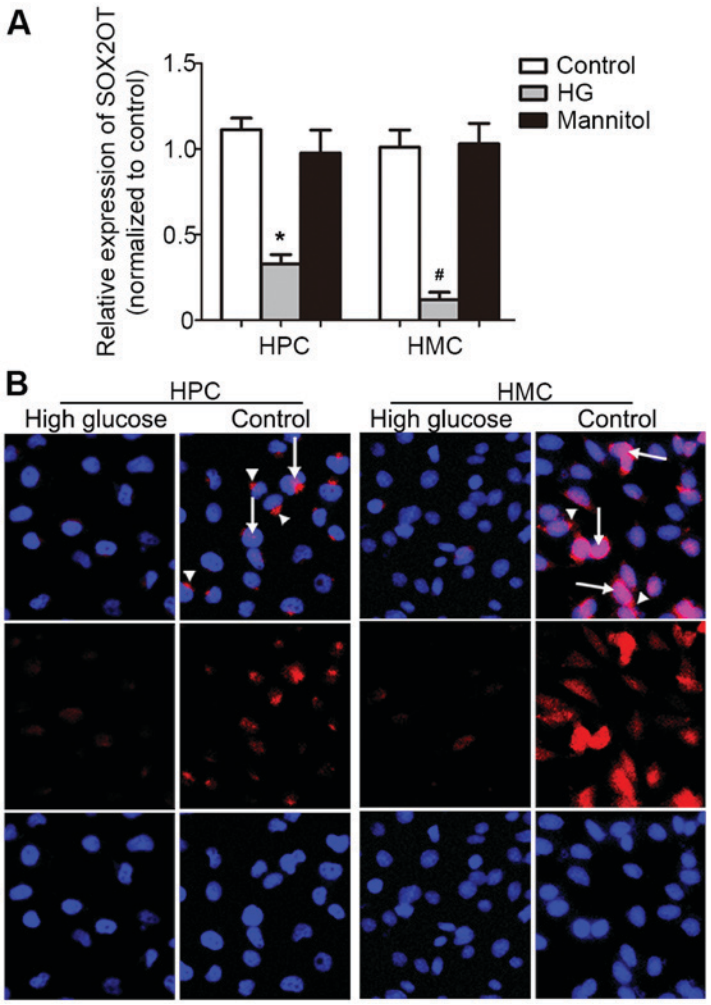

Figure 6. Expression and location of SOX2OT in HPCs and HMCs. (A) HPCs and HMCs were cultured and stimulated by HG. Expression of SOX2OT was determined by reverse transcription quantitative polymerase chain reaction. Data are presented as the mean relative expression level ± standard deviation. *P=0.0006 vs. Control HPC; #P=0.0043 vs. Control HMC. (n=3). (B) Fluorescence *in situ* hybridization was performed in cultured HPCs and HMCs. Arrows indicate that SOX2OT was expressed in the nucleus and the arrowhead indicates that it was expressed in the cytoplasm (magnification, x200). HPCs, human podocyte cells; HMCs, human mesangial cells; HG, high glucose treatment; SOX2OT, SOX2 original transcript.

SOX2OT expressed in the nucleus (arrow) and cytoplasm (arrow head). However, in HPCs, SOX2OT was expressed in the cytoplasm, while in HMCs, it was expressed in the nucleus. This very different distribution indicated that SOX2OT may have different roles in HPCs and HMCs under HG-stimulation.

Discussion

For decades, lncRNA has always been recognized as byproduct of the gene transcription. Although recent studies (23-25) have greatly improved current knowledge about the function and associated mechanism of lncRNA, it is mostly limited to the area of oncology. The role of lncRNA in renal diseases is largely unknown.

In the present study, db/db mice were used as a spontaneous diabetes model. Sustained high blood glucose ends in the occurrence of protein urea and finally the onset of DN. Microarray analysis using the renal cortex of db/db mice revealed large number of dysregulated lncRNAs and mRNAs. To investigate what biological processes and pathways were most altered GO and KEGG pathway enrichment analysis was carried out. As expected, metabolic associated biological processes were altered, including glucuronic associated processes. The significant cellular component enrichment of chylomicron was consistent with previous studies that demonstrated lipid dysregulation served an important role in DN (26,27). It is already well known that oxidative stress is associated with the onset and progression of DN (28). The present study's result also added novel evidence to the role of oxidative stress by describing alterations in certain known functional processes or pathways, including flavonoid-associated processes (29), cytochrome P450 (30) and glutathione metabolism (31). Alterations in other DN-associated pathways (32), including the renin-angiotensin system, PPAR signaling pathway and arachidonic acid metabolism were also demonstrated in the present study. These discoveries, on one hand, proved the successful establishment of the DN model at the molecular level and on the other hand they provided a whole picture of disordered gene expression, which indicates novel directions for future study. In addition, except for the commonly enriched pathways, steroid-related alterations were also demonstrated in GO and pathway enrichment maps. At present, steroids are widely used for treatment of diverse glomerular diseases. Although advanced stages of DN are often accompanied by

massive proteinuria, steroid hormones are rarely used in these patients due to side effects or uncertain effectiveness. However the results of the present study, together with other microarray analysis (33) suggested that steroid hormone disorders may also participate in the onset of DN, which requires further study in the future.

As is currently known, the common way for lncRNA to function is via interacting with mRNA. In the present study, the lncRNA-associated mRNA alterations were also discussed which could help prediction of the lncRNA-associated cellular functions. In the present study, the correlation of differentially expressed lncRNAs and mRNAs were presented as networks according to calculated PC values.

RT-qPCR was introduced to validate microarray results and a total of 10 lncRNAs and mRNAs were included. In these lncRNAs, PVT1 and SOX2OT have already been reported and researched in humans, especially in cancer (20,21). PVT1 has also been studied intensively in DN (34). However, the function of SOX2OT in DN has not been identified. Therefore, in the following studies, the role of SOX2OT was focused on in DN. GO enrichment was carried out again using co-expressed mRNAs of SOX2OT. As expected, enrichment results were highly consistent with GO and KEGG results. Flavonoid associated processes, oxidoreductase reaction, glutathione metabolism and steroid metabolic processes were all exhibited, indicating that SOX2OT is involved in the major disorders of DN. Since the role of SOX2OT in DN has not been reported previously, it is of interest to investigate the exact function, which may provide a novel point of view on DN treatment.

The location within the genome of SOX2OT is chromosome 3 in humans and mice. Conservational analysis demonstrated that SOX2OT is conserved in multiple vertebrates. This conservation among species indicated that SOX2OT may have an important role in normal physiology. SOX2OT has a number of variants (35). At least 6 versions were documented in NCBI. A total of three TSSs were demonstrated to start transcription of different variants. However, the overlapping sequences prevented the design of specific and highly efficient primers. As a result, only the total amount of SOX2OT was measured. SOX2OT was first reported to be associated with cell proliferation in breast cancer, lung cancer, colorectal cancer and gastric cancer (36-38). Su *et al* (39) proposed that SOX2OT acted as a microRNA (miR)-194-5p or miR-122 sponge and knockdown of SOX2OT inhibited the malignant biological behaviors of glioblastoma stem cell. Recently, it is reported that, in diabetes-induced retinal neurodegeneration, SOX2OT expression is significantly downregulated in the retinas of STZ-induced diabetic mice and in the Retinal Ganglion Cells upon HG or oxidative stress (40). Diabetic-induced nephropathy is also a micro-vascular complication and SOX2OT was also downregulated in the mice renal cortex and cultured HPCs and HMCs. FISH was performed to find out the cellular location. The images exhibited downregulation of SOX2OT under HG stimulation. Furthermore, it was demonstrated that the location of SOX2OT was very different in these two cells, suggesting that SOX2OT may serve different functions in different cells. Considering the conservation of SOX2OT between mice and humans, the consistent result of SOX2OT suggested it also plays a role in human DN. However, the role of SOX2OT in certain cell types needs further investigation.

In conclusion, the present study confirmed that db/db mice exhibited different gene expression compared with db/m mice and these DEGs were involved in diverse biological processes and pathways associated with DN. Out of these dysregulated lncRNAs, the significantly different and species-conserved lncRNA SOX2OT were identified to be the putative controller of DN onset and progression. SOX2OT may serve a central role in orchestrating scenarios of molecular disorder and be the putative target for DN treatment. The detailed function and role of SOX2OT in DN requires further study in the future.

Acknowledgements

Not applicable.

Funding

The present study was supported by the National Natural Science Foundation of China (grant nos. 81570690 and 81700633), the Excellent Youth Foundation of Henan Scientific Committee (grant no. 154100510017), the Youth Foundation of the First Affiliated Hospital of Zhengzhou University to Jin Shang, Key Scientific Research Projects of Henan Colleges and Universities (grant no. 17A320065), Foundation and Frontier Technology Research Program of Henan Province (grant no. 142300410211).

Availability of data and materials

The datasets used and/or analyzed during the current study are available from the corresponding author on reasonable request.

Authors' contributions

ZZ and JX conceived and designed the experiments; JS and XW performed the experiments; GC and DL analyzed the data; XZ and YJ analyzed and interpreted data and wrote the manuscript; ZZ revised and gave final approval of the manuscript to be published. All authors read and approved the final manuscript.

Ethics approval and consent to participate

All protocols were approved by the Institutional Animal Care and Use Committee of the First Affiliated Hospital of Zhengzhou University and conducted in accordance with the National Institutes of Health Guide for the Care and Use of Laboratory Animals.

Patient consent for publication

Not applicable.

Competing interests

The authors declare that they have no competing interests.

References

1. Vicente PC, Kim JY, Ha JJ, Song MY, Lee HK, Kim DH, Choi JS and Park KS: Identification and characterization of site-specific N-glycosylation in the potassium channel Kv3.1b. J Cell Physiol 233: 549-558, 2018.

2. Badal SS and Danesh FR: New insights into molecular mechanisms of diabetic kidney disease. Am J Kidney Dis 63 (2 Suppl 2): S63-S83, 2014.
3. Hwang SH, Han BI and Lee M: Knockout of ATG5 leads to malignant cell transformation and resistance to Src family kinase inhibitor PP2. J Cell Physiol 233: 506-515, 2018.
4. Frenette-Cotton R, Marcoux AA, Garneau AP, Noel M and Isenring P: Phosphoregulation of K(+) -Cl(-) cotransporters during cell swelling: Novel insights. J Cell Physiol 233: 396-408, 2018.
5. Shang J, Wan Q, Wang X, Duan Y, Wang Z, Wei X, Zhang Y, Wang H, Wang R and Yi F: Identification of NOD2 as a novel target of RNA-binding protein HuR: Evidence from NADPH oxidase-mediated HuR signaling in diabetic nephropathy. Free Radic Biol Med 79: 217-227, 2015.
6. Liu R, Liao X, Li X, Wei H, Liang Q, Zhang Z, Yin M, Zeng X, Liang Z and Hu C: Expression profiles of long noncoding RNAs and mRNAs in post-cardiac arrest rat brains. Mol Med Rep 17: 6413-6424, 2018.
7. Liao Z, Zhao J and Yang Y: Downregulation of lncRNA H19 inhibits the migration and invasion of melanoma cells by inactivating the NFkappaB and PI3K/Akt signaling pathways. Mol Med Rep 17: 7313-7318, 2018.
8. Xu JH, Chang WH, Fu HW, Yuan T and Chen P: The mRNA, miRNA and lncRNA networks in hepatocellular carcinoma: An integrative transcriptomic analysis from Gene Expression Omnibus. Mol Med Rep 17: 6472-6482, 2018.
9. Li Z, Xu Y, Liu X, Nie Y and Zhao Z: Urinary heme oxygenase-1 as a potential biomarker for early diabetic nephropathy. Nephrology (Carlton) 22: 58-64, 2017.
10. Zhang Z, Cheng X, Yue L, Cui W, Zhou W, Gao J and Yao H: Molecular pathogenesis in chronic obstructive pulmonary disease and therapeutic potential by targeting AMP-activated protein kinase. J Cell Physiol 233: 1999-2006, 2018.
11. Guo J, Xiao J, Gao H, Jin Y, Zhao Z, Jiao W, Liu Z and Zhao Z: Cyclooxygenase-2 and vascular endothelial growth factor expressions are involved in ultrafiltration failure. J Surg Res 188: 527-536e2, 2014.
12. Tian F, Gu C, Zhao Z, Li L, Lu S and Li Z: Urinary Emmprin, matrix metalloproteinase 9 and tissue inhibitor of metalloproteinase 1 as potential biomarkers in children with ureteropelvic junction narrowing on conservative treatment. Nephrology (Carlton) 20: 194-200, 2015.
13. Kong XD, Shi HR, Liu N, Wu QH, Xu XJ, Zhao ZH, Lu N, Li-Ling J and Luo D: Mutation analysis and prenatal diagnosis for three families affected by isolated methylmalonic aciduria. Genet Mol Res 13: 8234-8240, 2014.
14. Zou Y, Li C, Shu F, Tian Z, Xu W, Xu H, Tian H, Shi R and Mao X: lncRNA expression signatures in periodontitis revealed by microarray: The potential role of lncRNAs in periodontitis pathogenesis. J Cell Biochem 116: 640-647, 2015.
15. Zhang S, Zhang Y, Wei X, Zhen J, Wang Z, Li M, Miao W, Ding H, Du P, Zhang W, *et al*: Expression and regulation of a novel identified TNFAIP8 family is associated with diabetic nephropathy. Biochim Biophys Acta 1802: 1078-1086, 2010.
16. Livak KJ and Schmittgen TD: Analysis of relative gene expression data using real-time quantitative PCR and the 2(-Delta Delta C(T)) method. Methods 25: 402-408, 2001.
17. Shi X, Xu Y, Zhang C, Feng L, Sun Z, Han J, Su F, Zhang Y, Li C and Li X: Subpathway-LNCE: Identify dysfunctional subpathways competitively regulated by lncRNAs through integrating lncRNA-mRNA expression profile and pathway topologies. Oncotarget 7: 69857-69870, 2016.
18. Chen X: KATZLDA: KATZ measure for the lncRNA-disease association prediction. Sci Rep 5: 16840, 2015.
19. Hu M, Wang R, Li X, Fan M, Lin J, Zhen J, Chen L and Lv Z: LncRNA MALAT1 is dysregulated in diabetic nephropathy and involved in high glucose-induced podocyte injury via its interplay with β-catenin. J Cell Mol Med 21: 2732-2747, 2017.
20. Wang C, Han C, Zhang Y and Liu F: LncRNA PVT1 regulate expression of HIF1alpha via functioning as ceRNA for miR199a5p in nonsmall cell lung cancer under hypoxia. Mol Med Rep 17: 1105-1110, 2018.
21. Tang X, Gao Y, Yu L, Lu Y, Zhou G, Cheng L, Sun K, Zhu B, Xu M and Liu J: Correlations between lncRNA-SOX2OT polymorphism and susceptibility to breast cancer in a Chinese population. Biomark Med 11: 277-284, 2017.
22. Shahryari A, Jazi MS, Samaei NM and Mowla SJ: Long non-coding RNA SOX2OT: Expression signature, splicing patterns, and emerging roles in pluripotency and tumorigenesis. Front Genet 6: 196, 2015.
23. Munschauer M, Nguyen CT, Sirokman K, Hartigan CR, Hogstrom L, Engreitz JM, Ulirsch JC, Fulco CP, Subramanian V, Chen J, *et al*: The NORAD lncRNA assembles a topoisomerase complex critical for genome stability. Nature 561: 132-136, 2018.
24. Zhang Y, Pitchiaya S, Cieslik M, Niknafs YS, Tien JC, Hosono Y, Iyer MK, Yazdani S, Subramaniam S, Shukla SK, *et al*: Analysis of the androgen receptor-regulated lncRNA landscape identifies a role for ARLNC1 in prostate cancer progression. Nat Genet 50: 814-824, 2018.
25. Hua JT, Ahmed M, Guo H, Zhang Y, Chen S, Soares F, Lu J, Zhou S, Wang M, Li H, *et al*: Risk SNP-mediated promoter-enhancer switching drives prostate cancer through lncRNA PCAT19. Cell 174: 564-575e18, 2018.
26. Wong R, Chen W, Zhong X, Rutka JT, Feng ZP and Sun HS: Swelling-induced chloride current in glioblastoma proliferation, migration, and invasion. J Cell Physiol 233: 363-370, 2018.
27. Bagheri V, Memar B, Momtazi AA, Sahebkar A, Gholamin M and Abbaszadegan MR: Cytokine networks and their association with Helicobacter pylori infection in gastric carcinoma. J Cell Physiol 233: 2791-2803, 2018.
28. Feng B, Yan XF, Xue JL, Xu L and Wang H: The protective effects of alpha-lipoic acid on kidneys in type 2 diabetic Goto-Kakisaki rats via reducing oxidative stress. Int J Mol Sci 14: 6746-6756, 2013.
29. Olli KE, Li K, Galileo DS and Martin-DeLeon PA: Plasma membrane calcium ATPase 4 (PMCA4) co-ordinates calcium and nitric oxide signaling in regulating murine sperm functional activity. J Cell Physiol 233: 11-22, 2018.
30. Noda S, Sumita Y, Ohba S, Yamamoto H and Asahina I: Soft tissue engineering with micronized-gingival connective tissues. J Cell Physiol 233: 249-258, 2018.
31. Lin W, Izu Y, Smriti A, Kawasaki M, Pawaputanon C, Bottcher RT, Costell M, Moriyama K, Noda M and Ezura Y: Profilin1 is expressed in osteocytes and regulates cell shape and migration. J Cell Physiol 233: 259-268, 2018.
32. Xu HZ, Cheng YL, Wang WN, Wu H, Zhang YY, Zang CS and Xu ZG: 12-Lipoxygenase inhibition on microalbuminuria in Type-1 and Type-2 diabetes is associated with changes of glomerular angiotensin II Type 1 receptor related to insulin resistance. Int J Mol Sci 17: pii: E684, 2016.
33. Chen S, Dong C, Qian X, Huang S, Feng Y, Ye X, Miao H, You Q, Lu Y and Ding D: Microarray analysis of long noncoding RNA expression patterns in diabetic nephropathy. J Diabetes Complications 31: 569-576, 2017.
34. Alvarez ML and Distefano JK: The role of non-coding RNAs in diabetic nephropathy: Potential applications as biomarkers for disease development and progression. Diabetes Res Clin Pract 99: 1-11, 2013.
35. Strippoli R, Loureiro J, Moreno V, Benedicto I, Lozano ML, Barreiro O, Pellinen T, Minguet S, Foronda M, Osteso MT, *et al*: Caveolin-1 deficiency induces a MEK-ERK1/2-Snail-1-dependent epithelial-mesenchymal transition and fibrosis during peritoneal dialysis. EMBO Mol Med 7: 357, 2015.
36. Askarian-Amiri ME, Seyfoddin V, Smart CE, Wang J, Kim JE, Hansji H, Baguley BC, Finlay GJ and Leung EY: Emerging role of long non-coding RNA SOX2OT in SOX2 regulation in breast cancer. PLoS One 9: e102140, 2014.
37. Hou Z, Zhao W, Zhou J, Shen L, Zhan P, Xu C, Chang C, Bi H, Zou J, Yao X, *et al*: A long noncoding RNA Sox2ot regulates lung cancer cell proliferation and is a prognostic indicator of poor survival. Int J Biochem Cell Biol 53: 380-388, 2014.
38. Liu S, Xu B and Yan D: Enhanced expression of long non-coding RNA Sox2ot promoted cell proliferation and motility in colorectal cancer. Minerva Med 107: 279-286, 2016.
39. Su R, Cao S, Ma J, Liu Y, Liu X, Zheng J, Chen J, Liu L, Cai H, *et al*: Knockdown of SOX2OT inhibits the malignant biological behaviors of glioblastoma stem cells via up-regulating the expression of miR-194-5p and miR-122. Molecular cancer 16: 171, 2017.
40. Li CP, Wang SH, Wang WQ, Song SG and Liu XM: Long Noncoding RNA-Sox2OT knockdown alleviates diabetes mellitus-induced retinal ganglion cell (RGC) injury. Cell Mol Neurobiol 37: 361-369, 2017.